Metallomics



COMMUNICATION



Cite this: Metallomics, 2017, 9, 1735

Received 11th August 2017, Accepted 15th November 2017

DOI: 10.1039/c7mt00232g

rsc.li/metallomics

Sm(III)[12-MC_{Ga(III)shi}-4] as a luminescent probe for G-quadruplex structures†

Ewa Rajczak, Vincent L. Pecoraro o and Bernard Juskowiak **

G-quadruplexes (GQs), spatial assemblies of guanine-rich DNA strands, play an important role in the regulation of gene expression and chromosome stabilization. These structures are recognized to be useful in cancer therapies as the presence of multiple G-quadruplexes in a telomeric strand stops cancer cell proliferation. Metallacrowns of the type 12-MC-4 form planar structures that have remarkable similarity to G-tetrads in terms of dimension, shape and the ability to bind alkali metal and lanthanide cations in a central cavity. The interaction between the Sm(III)[12-MC_{Ga(III)shi}-4] (SmMC) metallacrown (MC) and human telomeric G-quadruplex structures was examined using several methods including CD titrations, CD melting temperatures, fluorescence titration of SmMC with GQ/Na⁺, fluorescence intercalator displacement (FID) assays and methods measuring the MC quenching effect on the Tb³⁺/GQ luminescence. It was proven that the studied metallacrown acted as a sensing probe and interacted with quadruplex DNA. The Stern-Volmer quenching constant (Kas) of Tb3+/GQ luminescence was calculated to be $3.9\times 10^5\;\text{M}^{-1}.$ The binding constant using the indirect FID method gave the result of 1.3 \times 10⁵ M⁻¹. CD melting temperature experiments reveal the following pattern - the higher the concentration of the complex the lower the registered $T_{\rm m}$ for quadruplex DNA, which indicates a destabilizing effect of SmMC at higher GQ: MC ratios. These data implicate a shape and size selective interaction between MCs and GQs that may be exploited for telomere detection.

Introduction

Among various DNA structures, tetraplexes are recognized as scaffolds that play a substantial role in every living organism. G-quadruplexes (GQs) are nucleic acid secondary structures, formed by guanine-rich sequences, for example, telomeric repeats. The first report about GQs with provided X-ray analysis

Significance to metallomics

This manuscript is focused on interactions between a Sm(III)/Ga(III)-based metallacrown (SmMC) and human telomeric G-quadruplex (GQ) structures. This higher-order DNA conformation is recognized as a target in cancer therapies. With several assays, we revealed that Sm(III)[12-MCGa(III)shi-4], which has a similar size and shape to a G-tetrad, interacted with quadruplex DNA and could be used as a fluorescent probe for biomedical applications. The GQ binding affinity and sensitivity of SmMC emission to higher temperatures and light are potentially promising for biosensing applications. This research reports the first example of a luminescent metallacrown compound that interacts with a planar guanine tetrad of a G-quadruplex.

was published in 1962. The human telomeric DNA bears runs of -TTAGGG- repeats that can be easily folded into G-quadruplexes. Four guanines form a planar tetrad with Hoogsteen-type base pairing. Association of these layers creates a spatial assembly stabilized by several cations, in particular sodium and potassium ions.^{2,3} These structures have been visualized *in vivo* with the use of fluorescent binding ligands.⁴ Some fluorescent compounds were even suggested for a visual detection of cell carcinogenic transformation.^{5,6} It was postulated that the existence of G-quadruplex structures on the telomeric strand may inhibit the activity of telomerase, the enzyme responsible for cancer cell proliferation. Moreover, clearly identified guanine-rich sequences able to adopt GQ folding are localized in some oncogenic promoters.^{3,8} Thus, the development of tools that enable recognition and manipulation of the quadruplex structures remains of great interest. A wide range of organic compounds have been reported as binding ligands for tetraplex DNA9 and metal complexes have also been considered as potential anticancer drugs.10 Lanthanide complexes were successfully examined as highly efficient luminescent probes¹¹ and sensors for targeting specific DNA structures. 12 Among these lanthanide containing species one can distinguish supramolecular sensors, which are based on lanthanide complexes/chelates. 13,14 Apart from that, lanthanide compounds were successfully used in

^a Faculty of Chemistry, Adam Mickiewicz University in Poznan, Umultowska 89b, 61-614 Poznan, Poland. E-mail: juskowia@amu.edu.pl

^b Chemistry Department, University of Michigan, Ann Arbor, MI 48109-1055, USA † Electronic supplementary information (ESI) available. See DOI: 10.1039/ c7mt00232g

structural biology¹⁵ and as MRI contrast agents.¹⁶ A new very promising class of lanthanide supramolecular complexes are metallacrowns.

Briefly, metallacrowns (MCs) are inorganic analogues of crown ethers, with the first literature report published in 1989. The Metallacrowns can vary in size, number and type of incorporated ions and organic ligands.¹⁸ A couple of broad reviews examine the evolution of metallacrowns and their properties. 19-22 The scaffold of the metallacrown is created with repeated motifs of [M-N-O] units. Each type can be written in the general formula of M(n) X-MC_{Mi(n)I-}Y, where M(n) is the central ion, X is the number of atoms that create the metallacrown scaffold (ring) and Y is the number of oxygen atoms oriented toward the central ion. Mi(n) and L stand for ring metal atoms and the ligand incorporated into the MC scaffold, respectively. In our previous report we described the interaction of the Ln(III)15-MC_{Cu(II)pheHA}-5 type metallacrowns with human telomeric G-quadruplex structures.²³ These compounds were shown to destabilize the higher-order DNA structure. They possessed an Eu³⁺ or Tb³⁺ ion incorporated in the central cavity and Cu²⁺ ions as ring metal cations. Although these lanthanide ions are often endowed with luminescence properties in the visible range, we could not observe emission in aqueous solution due to the quenching effect of unoccupied d orbitals of the copper(II). Thus, the metallacrown-DNA interactions were studied using indirect methods.

Herein, we are focusing on a different system – a 12-MC-4 type complex, in which four Ga3+ ions constitute the ring metals and their incorporation enhanced the fluorescence properties of the metallacrown.²⁴ In the investigated metallacrown, a samarium ion is located inside the centre of the scaffold and salicylhydroxamic acid (H₃shi) is applied as an organic antenna. The composition of the metallacrown is represented by the abbreviated formula of Sm(III)[12-MCGa(III)shi-4] (SmMC) and its molecular structure is presented in Fig. 1. This compound was recently reported;²⁴ however, bioanalytical studies (or applications) were not undertaken. Previously described 12-MC-4 complexes were identified as fungicides or as agents with antibacterial activity.25,26 Another communication reported that metallacrowns $[9\text{-MC}_{\text{CuN(PhPyCNO)}}\text{-}3]_2^{27}$ or Ln(III) 15-MC $_{\text{Cu(II)glyHa}}\text{-}5^{28}$ are able to interact with dsDNA via an intercalative binding mode. Nevertheless, all lanthanide metallacrowns investigated so far as DNA interacting ligands were non-fluorescent as their scaffold was created with the participation of paramagnetic transition metal ions (Cu(Π), Ni(Π), and Mn(Π)) that quench emission. Replacement of these d-block metals with Ga(III) allows for the development of strongly luminescent chromophores with the highest quantum yields for near IR emitting molecular species.²⁴

The crystal structure of SmMC revealed that the planarity of the 12-MC-4 ring is similar to that for Mn(III)/Ln(III) [12-MC_{Mn(III)Nshi}-4] and reminiscent of GQs.²⁹ This is an important consideration as this MC may be considered as a planar structure. Actually, in the SmMC complex the four Ga(III) ions bridged by four shi ligands possess a nearly planar geometry. In particular, the central Sm(III) ion is bridged to the ring metal ions by four benzoate ligands, which are perpendicular to the ring plane (Fig. 1C). The opposite side of the SmMC is exposed

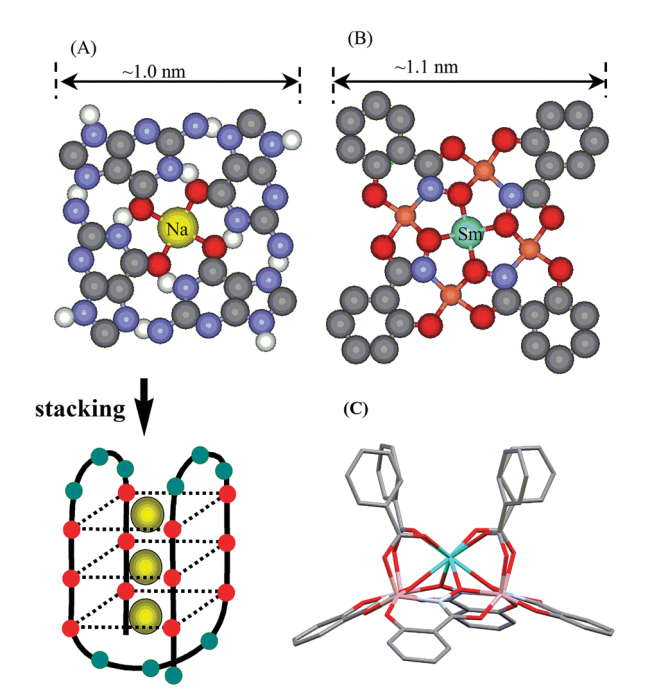


Fig. 1 (A) A ball and stick model of a G-tetrad with Hoogsteen-type base pairing and Na $^+$ cations coordinated in a central cavity. Tetrads assemble into a G-quadruplex structure as a result of stacking interactions. (B) A simplified molecular structure of Sm(III)[12-MC $_{\rm Ga(III)shi}$ -4]. The solvent molecules and benzoate bridging ligands have been omitted for clarity. Notice the similarity in shape, size, and cation binding of the two structures. (C) A side view of the Sm(III)/(benzoate)_4[12-MC $_{\rm Ga(III)shi}$ -4]. The metallacrown encapsulates a central samarium ion with four gallium ions (ring metal), four salicylhydroxamates (shi 3 -), and four benzoate bridges.

for the interaction with the terminal G-tetrad in a GQ. When one considers the relative edge length of the square generated by the MC (~ 11 Å) and compares this to the edge length of a G-tetrad (~ 10 Å), one sees striking size and shape complementarity (Fig. 1A and B). Furthermore, both MCs and GQs are capable of binding trivalent lanthanides or monovalent alkalications in the central core. Thus, the 12-MC-4 structure type provides a unique opportunity to exploit size, shape and cation binding similarities for precise molecular recognition of GQs (Fig. 1).

Herein, we present binding studies of the luminescent $Sm(III)[12\text{-}MC_{Ga(III)Shi}-4]$ metallacrown with a human telomeric G-quadruplex. CD spectra and fluorescence measurements were exploited to prove the binding affinity of SmMC to tetraplex DNA.

Materials and methods

All experimental details are described in the ESI.†

Results and discussion

UV-Vis absorption and fluorescence spectra

UV-Vis absorption spectra of SmMC are shown in Fig. 2A. The broad absorption band at 309 nm is connected with $\pi \to \pi^*$ transition in the shi ligand. In methanol solution, the metallacrown

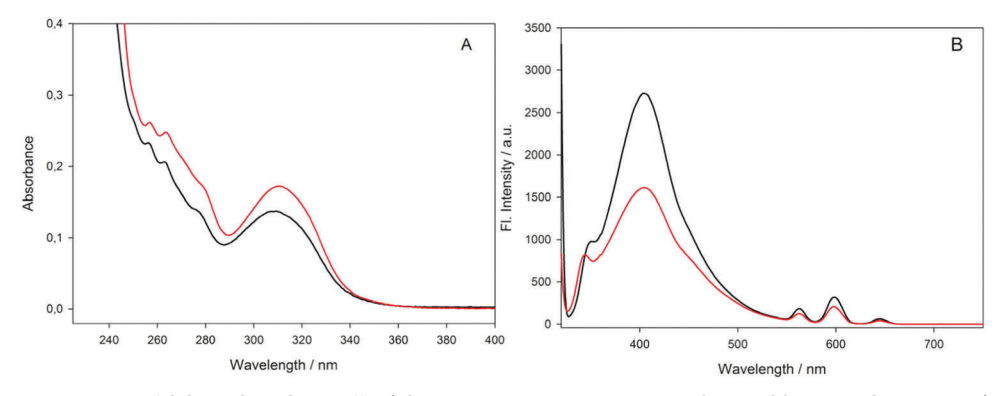


Fig. 2 (A) The absorption spectra of 8.8 μ M SmMC in buffer (10 mM sodium cacodylate, pH 7.2 and 100 mM NaCl, black line) and in the methanol solution (red line). (B) The emission spectra of 8.8 μ M SmMC in buffer (black line) and in methanol solution (red line). Parameters: λ_{ex} = 309 nm, excitation and emission slit widths both at 10 nm, sensitivity: medium.

exhibits a higher molar absorption coefficient ($\varepsilon_{\text{MeOH}}$ = $1.94 \times 10^4 \text{ M}^{-1} \text{ cm}^{-1}$) than that in buffer solution ($\varepsilon_{\text{H}_2\text{O}}$ = $1.51 \times 10^4 \, \mathrm{M^{-1} \, cm^{-1}}$). The presented results in methanol are in reasonable agreement with literature data ($\varepsilon_{\rm MeOH}$ = 2.16 imes $10^4 \,\mathrm{M}^{-1} \,\mathrm{cm}^{-1}$ at 311 nm). ²⁴ Emission spectra of 8.8 $\mu\mathrm{M}$ SmMC are presented in Fig. 2B. Spectra in MeOH and aqueous cacodylate buffer solutions are similar in shape but different in intensities. The broad emission band centered at around 400 nm reflects the fluorescence of the aromatic salicylhydroxamate ligand and two narrow bands at 558 and 594 nm are assigned to the luminescence of samarium incorporated into the metallacrown structure. A significant effect of the solvent on the nature of the emission properties of SmMC is seen. The positions of the emission bands remained unaffected; however, the intensity of the ligand band at ca. 400 nm for aqueous and methanol solutions differed markedly. The fluorescence intensity for SmMC in methanol was roughly half of that for aqueous solution. This rather odd solvent effect appeared to arise from a light-sensitive fluorescence of the metallacrown in aqueous solution (vide infra). Interestingly, samarium luminescence bands were not so much affected by medium replacement, which indicated that the samarium ion is protected from the quenching interaction with OH oscillators and consequently, that the SmMC complex remained intact in aqueous solution without a noticeable disassembly due to a dissociation process.

Circular dichroism (CD) study

The 22Htel oligonucleotide in the presence of Na $^+$ forms an anti-parallel GQ structure with two lateral loops and one diagonal loop, as depicted in Fig. 1A. This conformation is evidenced by a strong positive band at 295 nm and a negative ellipticity at 260 nm. 30 This particular structure was confirmed by crystallographic data 31 (143D code in Protein Data Bank). CD spectra of a 2 μM solution of G-quadruplex with varied concentrations of SmMC are presented in Fig. S1 (ESI $^+$). All CD spectra in Fig. S1 (ESI $^+$) exhibit two major bands as expected, a positive one at 295 nm and a negative one at 260 nm. Increasing the concentration of the metallacrown causes modest distortions in the G-quadruplex spectra. There is a lack of noticeable changes for the 260 and 295 nm bands when the GQ: MC ratios

are 1:2.3 and 1:6.9, which indicates that the G-quadruplex structure is negligibly affected by the interaction with MC. Nevertheless, at ratios 1:6.9 and higher, a small band at 240 nm that is also characteristic for anti-parallel quadruplexes, underwent significant reduction. It is not clear whether changes at this wavelength are related to conformational changes of the GQ or reflect artifacts connected with the presence of MC and scattering of polarized light on the cell walls.

To shed more light on this issue we recorded CD spectra of SmMC at different concentrations in the absence of GQ and the results are shown in Fig. S2 (ESI†). Basically, the SmMC complex is suspected to exist in two optical isomeric forms related to the ring connectivity (the M-N-O-M-N-O- linkage (A isomer) vs. the linkage M-O-N-M-O-N- (C isomer)). Nevertheless, because of the achiral synthetic protocol, the obtained product mixture should remain racemic and should not exhibit CD activity. However, it could be that to interact with GQ, one enantiomer is preferred over the other. This would generate an MC based CD signal. Unexpectedly, SmMC spectra in Fig. S2 (ESI†) showed weak negative bands at around 230 nm and 310 nm that corresponded to the absorption bands in the UV range. Although the shi ligand is not an optically active molecule, CD spectra of it revealed the same signals as observed for the metallacrown (data not shown). We are unable at present to find a reliable explanation of this observed effect.

To be able to see actual changes in the CD bands of the G-quadruplex structure, we applied a subtraction procedure. Appropriate CD spectra of the metallacrown itself (Fig. S2, ESI†) were mathematically subtracted from the CD spectra of the GQ/MC complex (Fig. S1, ESI†) and the results are shown in Fig. 3. One can conclude that the GQ structure is modestly affected at lower GQ: MC ratios but when the ratio approached a value of 1:12.4, the anti-parallel structure undergoes a noticeable conversion consistent with destruction of the anti-parallel assembly since the CD band intensities were reduced by about 40 and 30% at 295 and 260 nm, respectively (yellow line in Fig. 3).

It should be pointed out that the GQ showed remarkably higher stability in the presence of Sm12-MC-4 when compare with Ln15-MC-5 complexes, ²³ which is likely a consequence of a

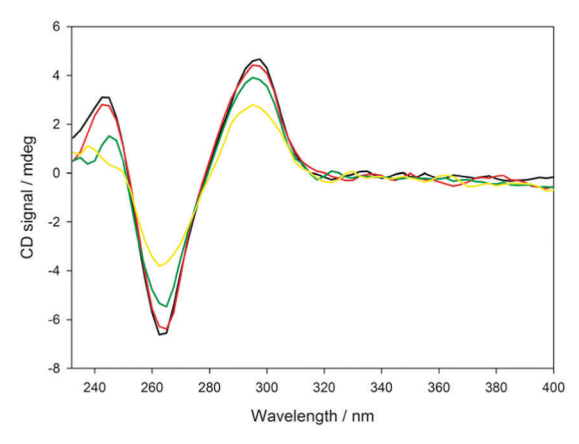


Fig. 3 CD spectra of the GQ/MC system obtained after subtraction of CD bands of SmMC in 10 mM sodium cacodylate buffer, pH 7.2 and 100 mM NaCl. Ratio GQ/MC equals 1:0 (black line), 1:2.3 (red dash), 1:6.9 (green line), and 1:12.4 (yellow line).

better fit between the GQ tetrad and 12-MC-4 plane, especially if one considers the high positive charge (+3) of Ln15-MC-5 that favors electrostatic interaction with the negatively charged DNA molecule. All these factors may suggest substantial differences between GQ binding modes for Ln12-MC-4 and Ln15-MC-5 complexes.

Effect of SmMC on the GQ melting behavior

Tracking the CD melting curve of the quadruplex during heating and cooling runs in the presence of an interacting compound should answer the question about the stabilization/destabilization effect of the metallacrown on the DNA structure. In a series of melting experiments with different GQ: MC ratios (1:0, 1:1, 1:2.3, 1:6.9 and 1:12.4), the thermal stability of each system was examined (Fig. 4). The thermal behavior of the G-quadruplex in the presence of the metallacrown was tracked

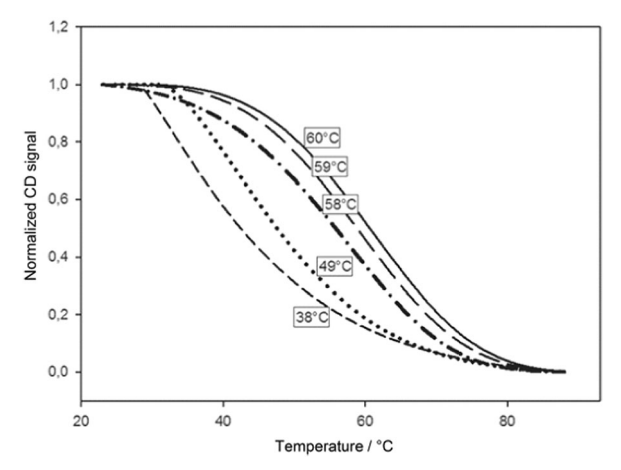


Fig. 4 Normalized melting profiles of 2 μ M G-quadruplex in the absence (solid line) and in the presence of the metallacrown at molar ratios: 1:1 (long dash line), 1:2.3 (dash-dot line), 1:6.9 (dotted line), and 1:12.4 (short dash line). Profiles were plotted using normalized CD signals at 295 nm vs. temperature. Conditions: 10 mM sodium cacodylate buffer, pH 7.2, 100 mM NaCl.

Table 1 Values of melting temperature for the 22Htel quadruplex obtained in the presence of varying GQ/MC ratios (mean values \pm SD of three determinations). Conditions: 2 μM GQ, 10 mM sodium cacodylate buffer, pH 7.2, 100 mM NaCl

$T_{ m m} \ [^{\circ} m C]$	$\Delta T_{\mathrm{m}} [^{\circ}\mathrm{C}]$
60 ± 2	0
59 ± 2	-1
58 ± 2	-2
49 ± 1	-11
38 ± 2	-22
	$60 \pm 2 59 \pm 2 58 \pm 2 49 \pm 1$

at 295 nm. Melting profiles at every ratio were registered in the cooling and heating approach. Melting temperatures (T_m) determined from heating cycles are presented in Table 1. The $T_{\rm m}$ value for the G-quadruplex in the absence of SmMC was determined to be 60 °C, in reasonable agreement with literature data.³² At ratios of 1:1 and 1:2.3, slightly lower values were obtained of 59 and 58 °C, respectively. In the case of both higher concentrations of SmMC (GQ: MC = 1:6.9 and 1:12.4), the melting temperature decreased by 11 °C and 22 °C, respectively, as compared to the GQ melting temperature without SmMC. In the cooling approach (85 \rightarrow 15 $^{\circ}$ C) we did not obtain overlapping melting profiles for the SmMC-containing samples, which suggested the presence of irreversible or very slow processes connected with the folding of the GQ/SmMC system. One possible reason for the observed hysteresis in melting plots can be associated with the temperature effect on the integrity of SmMC, which may undergo dissociation into components at higher temperature. Indeed, emission spectra recorded upon heating/cooling experiments with SmMC alone revealed that a temperature increase above ca. 75 °C caused thermal dissociation of the MC complex (Fig. S3, ESI†), which was manifested by enhancement of the emission band of the shi ligand by over 2 times ($\sim 200\%$), whereas the luminescence bands of samarium gradually disappeared. Moreover, the tendency of these spectral changes was further continued during the cooling cycle. Disruption of the SmMC complex at higher temperature appeared to be irreversible and metal cations or cationic complexes released from the metallacrown bound to DNA and prevented the oligonucleotide from folding into the proper GQ conformation. The interactions of nucleobases and DNA phosphate groups with cationic products of MC thermal dissociation were probably responsible for disturbing the GQ folding.

Comparing the results from the melting experiments with the CD spectra (Fig. 3), one can notice apparent discrepancies, especially at a ratio of 1:6.9. A higher impact on the G-quadruplex structure at this MC:GQ ratio is observed in the melting temperature experiment (a decrease in $T_{\rm m}$ of 11 °C), whereas the CD spectrum did not exhibit such a dramatic change. Thus, it is highly likely that the increased temperature triggers further loss of benzoates from the MC complex (generation of positively charged species after benzoate dissociation), which, when the SmMC is in excess, causes the released positively charged complexes to inhibit the G-quadruplex folding.

Taking into account all CD-based results one can conclude that at higher MC concentration, when the π - π stacking interactions of guanine quartets with the MCs have been saturated (end-stacking mode), the interactions between the DNA phosphate groups and metallacrown complexes may lead to a new external binding mode that can destabilize the GQ antiparallel structure.

Fluorescence titration of SmMC with GQ/Na⁺ quadruplex

Contrary to copper(II) that quenches lanthanide luminescence in MC systems, ²³ Ga³⁺ ions with fully occupied 3d orbitals do not disturb the luminescence transitions in lanthanide ions.²⁴ Moreover, the spatial architecture of SmMC protects the samarium ion from CH and OH oscillator quenching, giving a strong luminescence enhancement effect. Since we observed an odd solvent effect and low reproducibility of the recorded emission spectra for the aqueous solution of SmMC, more systematic experiments were carried out to clarify this point. Fig. 5 shows emission spectra of 1 μ M SmMC in buffer solution collected repeatedly after each 4 min (total incubation time of 56 min). Each subsequent scan (xenon lamp irradiation at $\lambda_{\rm ex}$ = 309 nm, cycles of 4 min) revealed a gradual increase in the 405 nm emission band (totally 5 times) and simultaneous decrease in the luminescence bands of samarium (inset in Fig. 5). The similarity of the observed spectral changes to the temperature effect seen in the melting studies (Fig. S3, ESI†) suggests operation of a light-induced dissociation of components (such as the benzoates) of the metallacrown. The observed coupling of ligand fluorescence (enhancement) with Sm(III) emission (quenching) indicates that energy transfer from the shi ligand to the central samarium ion is responsible for Sm(III) luminescence. One can suspect that shi excitation and energy transfer may activate oscillation of bonds within the coordination sphere of Sm(III), which facilitates the release of benzoate ligands and an attack of water molecules causing quenching of the SmMC luminescence. Such a process may lead to the

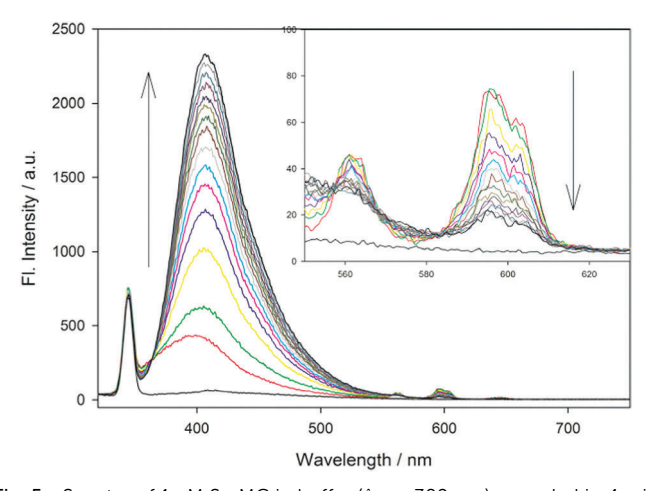


Fig. 5 Spectra of 1 μ M SmMC in buffer (λ_{ex} = 309 nm) recorded in 4 min time intervals. Arrows indicate intensity changes in emission bands with time. The inset shows detailed changes in the spectral region of samarium luminescence.

irreversible disassembly of SmMC. To assess the validity of such a pathway, we examined the reversibility of the SmMC photo-behavior by recording 4 min time profiles for emission of SmMC in buffer (at 405 nm and 596 nm) interrupted with 2 min dark intervals. The results are shown in Fig. S4 (ESI†). Continuous irradiation of SmMC in buffer caused a rapid increase in fluorescence (405 nm) and a slow reduction of Sm(III) luminescence. However, after a 2 min relaxation period without irradiation, subsequent scans started from an intensity that was close to the initial level of the first trace. Repeated scans for samarium luminescence also showed reversibility, but less pronounced than for the fluorescence traces. The results shown in Fig. S4 (ESI†) indicate at least partial reversibility of the photo-induced dissociation processes in SmMC and exclude total dissociation of the metallacrown. This observation is consistent with previous studies that demonstrated that while 12-MC-4 complexes may dissociate coordinated anions, the metallacrown ring and centrally captured metal are robust to dissociation or decomposition.33-38 The above explanation of the light-dependent increase of SmMC fluorescence agrees with reports concerning photochemical reactivity of some hydroxamic derivatives. Reversible oscillating photoreactions that caused fluorescence enhancement were reported for aromatic hydroxamate derivatives.³⁹ In our case, the shi ligand-centered photoreaction probably affects coordination bonds around Sm(III) and enables quenching by water molecules. There is a close correlation of the observed light effect on MC emission changes with the temperature discussed above (Fig. S3, ESI†). However, in melting experiments the extent of SmMC decomposition seems to be much higher since thermal dissociation is enhanced by photoreaction induced by light. At room temperature, SmMC dissociation appeared to be limited to the loss of benzoate ligands without the loss of metallacrown ring integrity. In contrast to fluorescence changes, results from a similar UV-Vis absorption experiment showed absorbance changes of only ca. 2% (Fig. S5, ESI†).

Considering the above effect, the direct study of binding interactions of samarium MC with nucleic acids using a fluorescence technique seemed to be rather problematic. Nevertheless, to estimate the GQ effect on the SmMC photo-behavior, one can compare the fluorescence plot of SmMC titrated with GQ in buffer with the reference titration performed with buffer only. Titration plots showing emission changes at ligand and samarium bands are compared in Fig. 6. Significant differences can be observed between GQ and reference titration plots monitored at the ligand fluorescence band (Fig. 6A), whereas for samarium emission traces the difference is not so evident (Fig. 6B). We conclude that the interaction (binding) of SmMC with GQ resulted in partial protection of SmMC from the light effect as can be inferred from the smaller increase in ligand fluorescence for GQ titration. We have carried out another titration experiment with a narrowed excitation slit to minimize light effects on the SmMC and to obtain more reliable GQ-binding results. Titration spectra of this experiment are shown in Fig. 7A and emission changes at the samarium band are plotted in Fig. 7B together with the corresponding reference

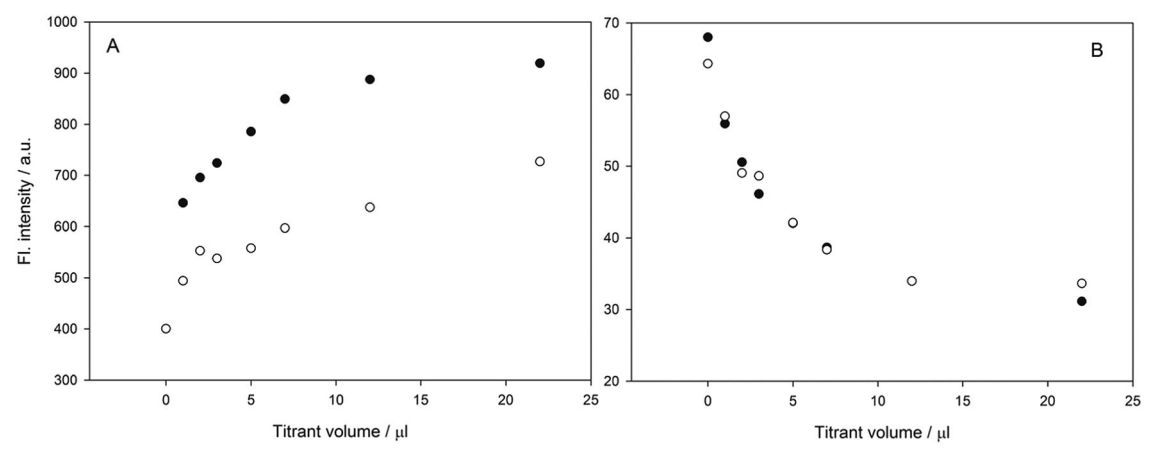


Fig. 6 Titration plots of 1 μ M SmMC monitored by ligand fluorescence at 405 nm (A) and by samarium luminescence at 596 nm (B) for GQ titration (white circle) and reference titration with buffer (black dots). Conditions: 10 mM sodium cacodylate buffer, pH 7.2, 100 mM NaCl. Parameters: λ_{ex} = 309 nm, ex. slit 5 nm, em. slit 5 nm, sensitivity: high.

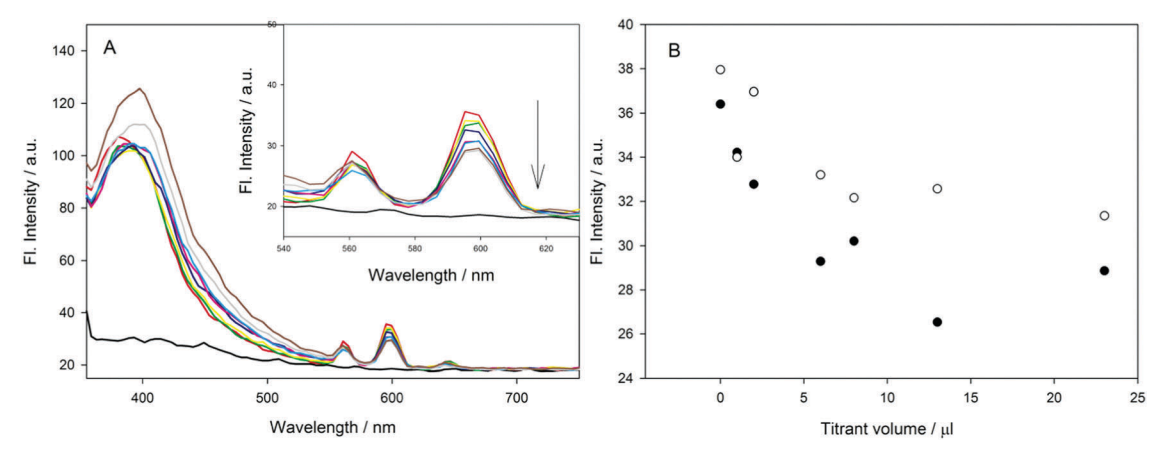


Fig. 7 (A) The emission spectra of 1 μ M SmMC (red line) titrated with increasing concentration of G-quadruplex (λ_{ex} = 309 nm). The arrows indicate the direction of intensity changes with increasing concentration of GQ [0–1.5 μ M]. The inset shows detailed changes in the spectral region of samarium luminescence. (B) Titration plot of SmMC monitored by samarium luminescence at 596 nm for GQ titration (open circles) and reference titration with buffer (black circles). Conditions: 10 mM sodium cacodylate buffer, pH 7.2, 100 mM NaCl. Parameters: λ_{ex} = 309 nm, ex. slit 2.5 nm, em. slit 5 nm, sensitivity: high.

titration plot. In contrast to the previous results (Fig. 6), initial additions of GQ (0.67 \times 10⁻⁷ to 0.54 \times 10⁻⁶ M) caused modest spectral effects (small fluorescence band shifts to longer wavelengths and fluorescence decrease), but at GQ concentrations of 0.9 µM and higher, the fluorescence intensity of the ligand band noticeably increased. Reference titrations with buffer additions imposed negligible changes in the fluorescence intensity at 405 nm. Fig. 7B shows the GQ titration plot monitored with samarium luminescence (open circles). Compared to the result of the reference titration (with buffer only) one can notice that the binding of SmMC to GQ protects the metallacrown from lightinduced luminescence quenching. These results indicate that the conclusions concerning the photoinduced decrease of samarium emission and complex integrity may be valid only under specific experimental conditions. This issue requires further study to resolve the mechanism of the photo-process that takes place in the SmMC chromophore. Due to the above discussed peculiar results, the fluorescent titration approach provided qualitative

but not quantitative evidence for the interaction between SmMC and GQ.

Tb/GQ quenching experiment

To confirm the interaction of SmMC with quadruplex DNA, we applied an indirect method based on the quenching effect of the ligand on the luminescence of the GQ/Tb³⁺ system. The design of this experiment was guided by the literature data concerning the relatively high apparent stability constant between Tb³⁺ ions and G-quadruplex ($K_b = 5 \times 10^6 \text{ M}^{-1}$). It was proven that this lanthanide ion was able to bind to DNA and an efficient energy transfer occurred from the nucleobase donor to the terbium ion acceptor. This effect was manifested by increased Tb luminescence bands and was already exploited in bioanalytical applications. $^{12-14}$

Luminescence spectra of the GQ/Tb³⁺ system titrated with increasing concentration of SmMC are presented in Fig. 8A. At the beginning of the experiment, the strong Tb³⁺ luminescence

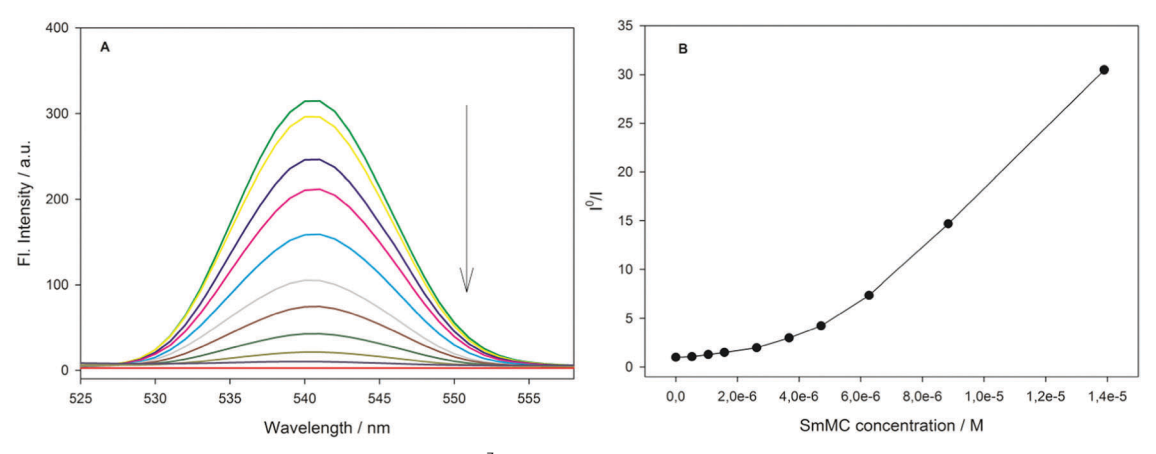


Fig. 8 (A) Quenching of the Tb(III) emission band of the $GQ-Tb^{3+}$ system by consecutive additions of SmMC. Experimental conditions: $[GQ] = 1 \mu M$, $[Tb^{3+}] = 4 \mu M$, $[MC] = 0-14 \mu M$; 10 mM Tris-HCl buffer, pH 7.0; $\lambda_{ex} = 290$ nm. Arrows indicate increasing concentration of metallacrown. (B) Plot of I^0/I versus increasing concentration of metallacrown.

band at 540 nm is visible (green line). Consecutive additions of metallacrown (up to 14 µM) diminished this band gradually. The observed effect provides evidence for the interaction of the metallacrown with the GQ/Tb³⁺ complex. A Stern-Volmer plot is presented in Fig. 8B. The plot of I^0/I versus metallacrown concentration showed an upward curvature. Interestingly, the positive deviation of the quenching plot is observed at GQ: MC ratios of 1:6 or higher, which is consistent with gradual unfolding of the GQ assembly. The GQ destabilizing effect of SmMC at high concentration ratios (1:6.9 and 1:12.2) has been evidenced by the CD titration (Fig. 3). To calculate a Stern-Volmer constant (association constant for static quenching), we took into consideration only the linear part of the S-V plot $(0-3.6 \mu M)$. The initial linear part of the quenching plot reflects association of the MC to GQ but further upward curvature of the plot may be associated with GQ unfolding and, because of higher SmMC concentration, contains contribution from the inner filter effect. The determined Stern-Volmer quenching constant of 3.9 \pm 0.3 \times $10^5\,M^{-1}$ was similar to those obtained for 15-MC-5 species $-3.9 \times 10^5 \text{ M}^{-1}$ and $4.6 \times 10^5 \text{ M}^{-1}$ for Eu(III) and Tb(III) [15-MC_{Cu(II)pheHA}-5], respectively. The apparent similarity of the GQ binding constants for both 12-MC-4 and 15-MC-5 complexes might suggest that the interaction modes are the same, which we doubt to be true. The 15-MC-5 copper Ln complexes have a charge of +3, which facilitates interaction with the negatively charged DNA. In contrast, the SmMC is a monoanion, and thus it should be repelled from the DNA. The fact that a monoanionic complex associates with the GQ with a similar affinity as a trivalent cation indicates that there is a different mechanism for the interaction than just charge-based. It is likely that this difference is that the Sm12-MC-4 matches the size and shape of the G-tetrad and binds GQ by an end stacking mode, whereas the polycationic Ln15-MC-5 probably interacts with the negatively charged phosphates by Coulombic forces. One cannot exclude however for SmMC a mixed-mode binding, by the end stacking at low GQ/MC ratios followed by external interactions with phosphates (benzoate dissociation products).

Fluorescence intercalator displacement (FID) assay

The interaction between MC and GQ was examined using another indirect method - the G-quadruplex fluorescence intercalator displacement assay. 41,42 In this method the fluorescence signal of thiazole orange (TO) bound to G-quadruplex is measured upon titration with a competing ligand. Thiazole orange is a fluorescent dye, which free in aqueous solution possesses almost negligible quantum yield. However, when the molecule is bound to DNA, a highly enhanced emission is observed. After excitation at 480 nm the TO/GQ complex emits a signal at 530 nm (Fig. 9A). Every addition of SmMC (0–14 μ M) decreases the fluorescence of the TO-GQ system (the direction of changes is indicated by an arrow). The principle of the method assumes the replacement of TO by the competing compound (here, SmMC). The competition binding plot was drawn as the dependence of the TO displacement (in percentage) against metallacrown concentration (Fig. 9B). The metallacrown concentration required to reduce the TO/GQ fluorescence signal by 50% (MC_{50%}) was estimated to be 5.3 \pm 0.3 μ M.

The displacement result was substituted into eqn (3) in the ESI† to determine the binding constant of the metallacrown with quadruplex DNA. The calculated value of $1.3 \pm 0.2 \times 10^5$ M suggested a moderate binding affinity of SmMC to GQ.

The values of $MC_{50\%}$ and K_{MC} for $Ln(m)[15\text{-}MC_{Cu(II)pheHA}\text{-}5}]^{23}$ metallacrowns amounted to $2.7\text{-}3.4 \times 10^{-6} \text{ M}^{-1}$ and $1.9\text{-}2.5 \times 10^5 \text{ M}^{-1}$, respectively, indicating a higher binding affinity to the quadruplex structure. The binding constant of $1.3 \times 10^5 \text{ M}^{-1}$ determined from the FID assay is also lower than that obtained by Tb/GQ luminescence quenching $(3.9 \times 10^5 \text{ M}^{-1})$. But this apparent discrepancy can be explained by different experimental conditions in both assays. In contrast to the Tb/GQ quenching method that required low ionic strength, the FID experiment was carried out in the presence of 100 mM NaCl. It is well known that a high salt content lowers the binding affinities of ligands with DNA, especially if it reduces electrostatic interactions. Another factor that could increase the apparent binding constant is the excitation wavelength (290 nm) required

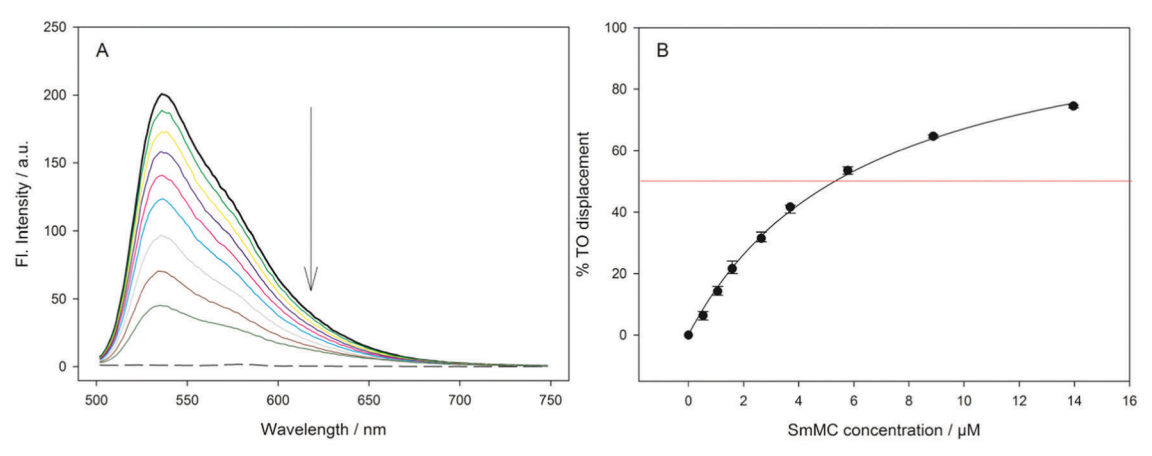


Fig. 9 (A) Spectra of $0.25~\mu M$ GQ containing $0.5~\mu M$ TO in the presence of increasing concentrations of MC in 10 mM sodium cacodylate buffer, pH 7.2 and 100 mM NaCl. (B) Plot of the TO displacement percentage against concentration of the metallacrown.

in the Tb/GQ quenching assay. Beside Tb/GQ excitation, this wavelength excited also the SmMC complex and, as discussed above, it induced photoreaction of SmMC causing alteration of the SmMC composition. Assuming the partial, or complete, dissociation of benzoate ligands from the SmMC and formation of positively charged complexes, one cannot exclude operation of a mixed mechanism of Tb/GQ quenching: by a monoanionic SmMC bound to the G-tetrad due to the end-stacking mode and by positively charged SmMC photo-products interacting non-specifically with anionic phosphates. The above described binding modes can be regarded as a general model of interaction between 12MC4 complexes and GQ. Therefore, the interaction of SmMC with GQ should be characterized by a range of binding constant with an upper/lower limit on the SmMC:GQ affinity of $3.9\text{--}1.3\times10^5~\text{M}^{-1}$.

Conclusions

The present study on the interaction of SmMC with the oligonucleotide bearing human telomeric sequence AG₃(TTAGGG)₃ indicated that this anionic metallacrown is able to form complexes with G-quadruplex DNA. This statement was confirmed with several methods based on direct and indirect measurements. Incorporation of gallium instead of copper ions endowed the metallacrown with luminescent properties; however, the fluorescence properties of the SmMC could not be directly exploited for calculation of the binding constant from titration experiments since the emission of SmMC appeared to be unstable and sensitive to the excitation. Observed spectral changes suggested light-induced dissociation of benzoate anions from the metallacrown in aqueous solution that led to quenching of the Sm emission. Nonetheless, fluorometric titration plots demonstrated the stabilizing effect of GQ on the decomposition of SmMC. The binding affinity of SmMC to GQ DNA was, therefore, further studied with indirect approaches. The MC quenching effect on the Tb3+/GQ luminescence and GQ FID assay indicated a moderate binding constant of SmMC with GQ in the range of $3.9 \times 10^5 \,\mathrm{M}^{-1}$ to $1.3 \times 10^5 \,\mathrm{M}^{-1}$, depending on the experimental conditions used. The impact of the MC on the quadruplex structure was observed in melting experiments. Higher GQ/MC ratios of 1:6.9 and 1:12.4 caused a decrease in the $T_{\rm m}$ value by 11 and 22 °C, respectively, compared to the initial G-quadruplex melting temperature of 60 °C. This GQ-destabilizing effect was less pronounced than the results obtained for Ln(III)[15-MC_{Cu(II)pheHA}-5].^{23} For 15-MC-5 type systems, the GQ:MC ratio of 1:10 yielded complete loss of quadruplex CD characteristic bands, whereas the CD spectrum of SmMC at the ratio of 1:12.4 still exhibited clearly visible G-quadruplex bands. This difference may reflect the proposed different binding interaction of the metallacrowns with GQ DNA. The 12-MC-4 interacted primarily through shape selective recognition whereas the tripositively charged species interacted primarily with the polyphosphate backbone of the nucleic acids.

The results presented in this paper indicated that $[12\text{-}MC_{Ga(III)shi}\text{-}4]$ metallacrown could be exploited as a fluorescent probe for G-quadruplex DNA and for other biomedical applications. The temperature and light effect of SmMC decomposition (release of metal cations) mediated by GQ is of particular interest. Complete characterization of the SmMC/DNA systems requires further systematic studies. Future studies using dimerized SmMCs that have been shown to be solution and photochemically stable may represent another attractive option for probing MC/GO interactions. 43

Conflicts of interest

The authors declare no conflict of interest.

Acknowledgements

The research has received funding from the National Science Centre of Poland, grant no. 2014/13/N/ST4/04099 and from the European Community's Seventh Framework Programme (FP7/2007-2013) under grant agreement no. 611488 (IRSES Metallacrowns) and the US National Science Foundation under grant (CHE-1664964).

References

- 1 M. Gellert, M. N. Lipsett and D. R. Davies, Helix formation by guanylic acid, *Proc. Natl. Acad. Sci. U. S. A.*, 1962, **48**, 2013–2018.
- 2 A. T. Phan, V. Kuryavyi and D. J. Patel, DNA architecture: from G to Z, *Curr. Opin. Struct. Biol.*, 2006, **16**, 288–298.
- 3 S. Burge, G. N. Parkinson, P. Hazel, A. K. Todd and S. Neidle, Quadruplex DNA: sequence, topology and structure, *Nucleic Acids Res.*, 2006, **34**, 5402–5415.
- 4 G. Biffi, D. Tannahill, J. McCafferty and S. Balasubramanian, Quantitative visualization of DNA G-quadruplex structures in human cells, *Nat. Chem.*, 2013, 5, 182–186.
- 5 T.-L. Yang, L. Lin, P.-J. Lou, T.-C. Chang and T.-H. Young, Detection of Cell Carcinogenic Transformation by a Quadruplex DNA Binding Fluorescent Probe, *PLoS One*, 2014, **9**, e86143.
- 6 T.-Y. Tseng, Z.-F. Wang, C.-H. Chien and T.-C. Chang, In-cell optical imaging of exogenous G-quadruplex DNA by fluorogenic ligands, *Nucleic Acids Res.*, 2013, 41, 10605–10618.
- 7 C. Philippi, B. Loretz, U. F. Schaefer and C. M. Lehr, Telomerase as an emerging target to fight cancer—opportunities and challenges for nanomedicine, *J. Controlled Release*, 2010, **146**, 228–240.
- 8 D. J. Patel, A. T. Phan and V. Kuryavyi, Human telomere, oncogenic promoter and 5'-UTR G-quadruplexes: diverse higher order DNA and RNA targets for cancer therapeutics, *Nucleic Acids Res.*, 2007, **35**, 7429–7455.
- 9 T-miao Ou, Y-jing Lu, J-heng Tan, Z-shu Huang, K.-Y. Wong and L-quan Gu, G-Quadruplexes: Targets in Anticancer Drug Design, *ChemMedChem*, 2008, 3, 690–713.
- 10 Q. Cao, Y. Li, E. Freisinger, P. Z. Qin, R. K. O. Sigel and Z.-W. Mao, G-quadruplex DNA targeted metal complexes acting as potential anticancer drugs, *Inorg. Chem. Front.*, 2017, 4, 10–32.
- 11 X. Wang, H. Chang, J. Xie, B. Zhao, B. Liu, S. Xu, W. Pei, N. Ren, L. Huang and W. Huang, Recent developments in lanthanide-based luminescent probes, *Coord. Chem. Rev.*, 2014, 273–274, 201–212.
- 12 C. Zhao, Y. Sun, J. Ren and X. Qu, Recent progress in lanthanide complexes for DNA sensing and targeting specific DNA structures, *Inorg. Chim. Acta*, 2016, **452**, 50–61.
- 13 J. L. Worlinsky and S. Basu, Detection of Quadruplex DNA by Luminescence Enhancement of Lanthanide Ions and Energy Transfer from Lanthanide Chelates, *J. Phys. Chem. B*, 2009, **113**, 865–868.
- 14 H. Xu, H. Zhang and X. Qu, Interactions of the human telomeric DNA with terbium-amino acid complexes, *J. Inorg. Biochem.*, 2006, **100**, 1646–1652.
- 15 G. Otting, Prospects for lanthanides in structural biology by NMR, *J. Biomol. NMR*, 2008, **42**, 1–9.
- 16 P. Caravan, Protein-Targeted Gadolinium-Based Magnetic Resonance Imaging (MRI) Contrast Agents: Design and Mechanism of Action, *Acc. Chem. Res.*, 2009, 42, 851–862.
- 17 M. S. Lah and V. L. Pecoraro, Isolation and characterization of {Mn^{II}[Mn^{III}(salicylhydroximate)]₄(acetate)₂(DMF)₆}. 2DMF: an

- inorganic analog of M²⁺ (12-crown-4), *J. Am. Chem. Soc.*, 1989, **111**, 7258–7259.
- 18 G. Mezei, C. M. Zaleski and V. L. Pecoraro, Structural and Functional Evolution of Metallacrowns, *Chem. Rev.*, 2007, **107**, 4933–5003.
- 19 C. Y. Chow, E. R. Trivedi, V. L. Pecoraro and C. M. Zaleski, Heterometallic Mixed 3d-4f Metallacrowns: Structural Versatility, Luminescence, and Molecular Magnetism, Comments Inorg. Chem., 2015, 35, 214–253.
- 20 M. Ostrowska, I. O. Fritsky, E. Gumienna-Kontecka and A. V. Pavlishchuk, Metallacrown-based compounds: Applications in catalysis, luminescence, molecular magnetism, and adsorption, *Coord. Chem. Rev.*, 2016, 327–328, 304–332.
- 21 P. Happ, C. Plenk and E. Rentschler, 12-MC-4 metallacrowns as versatile tools for SMM research, *Coord. Chem. Rev.*, 2015, **289–290**, 238–260.
- 22 M. Tegoni and M. Remelli, Metallacrowns of copper(II) and aminohydroxamates: Thermodynamics of self assembly and host-guest equilibria, *Coord. Chem. Rev.*, 2012, **256**, 289–315.
- 23 E. Rajczak, A. Gluszynska and B. Juskowiak, Interaction of metallacrown complexes with G-quadruplex DNA, *J. Inorg. Biochem.*, 2016, 155, 105–114.
- 24 C. Y. Chow, S. V. Eliseeva, E. R. Trivedi, T. N. Nguyen, J. W. Kampf, S. Petoud and V. L. Pecoraro, Ga³⁺/Ln³⁺ Metallacrowns: A Promising Family of Highly Luminescent Lanthanide Complexes That Covers Visible and Near-Infrared Domains, *J. Am. Chem. Soc.*, 2016, 138, 5100–5109.
- 25 I. Tsivikas, M. Alexiou, A. A. Pantazaki, C. Dendrinou-Samara, D. A. Kyriakidis and D. P. Kessissoglou, The Effect of Fused 12-Membered Nickel Metallacrowns on DNA and their Antibacterial Activity, *Bioinorg. Chem. Appl.*, 2003, 1, 85–97.
- 26 M. Alexiou, I. Tsivikas, C. Dendrinou-Samara, A. Pantazaki, P. Trikalitis, N. Lalioti, D. Kyriakidis and D. Kessissoglou, High nuclearity nickel compounds with three, four or five metal atoms showing antibacterial activity, *J. Inorg. Biochem.*, 2003, 93, 256–264.
- 27 A. Tarushi, C. P. Raptopoulou, V. Psycharis, C. K. Kontos, D. P. Kessissoglou, A. Scorilas, V. Tangoulis and G. Psomas, Copper(II) Inverse-[9-Metallacrown-3] Compounds Accommodating Nitrato or Diclofenac Ligands: Structure, Magnetism, and Biological Activity: Copper(II) Inverse-[9-Metallacrown-3] Compounds, *Eur. J. Inorg. Chem.*, 2016, 219–231.
- 28 Y. Meng, H. Yang, D. Li, S. Zeng, G. Chen, S. Li and J. Dou, Synthesis, crystal structure, DNA-binding and magnetism of copper 15-metallacrown-5 complexes based on glycine-hydroxamic acid ligand, *RSC Adv.*, 2016, **6**, 47196–47202.
- 29 M. R. Azar, T. T. Boron, J. C. Lutter, C. I. Daly, K. A. Zegalia, R. Nimthong, G. M. Ferrence, M. Zeller, J. W. Kampf, V. L. Pecoraro and C. M. Zaleski, Controllable Formation of Heterotrimetallic Coordination Compounds: Systematically Incorporating Lanthanide and Alkali Metal Ions into the Manganese 12-Metallacrown-4 Framework, *Inorg. Chem.*, 2014, 53, 1729–1742.
- 30 P. Balagurumoorthy and S. K. Brahmachari, Structure and stability of human telomeric sequence, *J. Biol. Chem.*, 1994, **269**, 21858–21869.

- 31 Y. Wang and D. J. Patel, Solution structure of the human telomeric repeat d [AG3 (T2AG3) 3] G-tetraplex, *Structure*, 1993, 1, 263–282.
- 32 J.-L. Mergny, A.-T. Phan and L. Lacroix, Following G-quartet formation by UV-spectroscopy, *FEBS Lett.*, 1998, 435, 74–78.
- 33 B. R. Gibney, D. P. Kessissoglou, J. W. Kampf and V. L. Pecoraro, Copper(II) 12-metallacrown-4: Synthesis, structure, ligand variability, and solution dynamics in the 12-MC-4 structural motif, *Inorg. Chem.*, 1994, 33, 4840–4849.
- 34 B. R. Gibney, H. Wang, J. W. Kampf and V. L. Pecoraro, Structural evaluation and solution integrity of alkali metal salt complexes of the manganese 12-metallacrown-4 (12-MC-4) structural type, *Inorg. Chem.*, 1996, 35, 6184–6193.
- 35 B. R. Gibney and V. L. Pecoraro, The Preparation of Manganese and Copper 12-Metallacrown-4 Complexes: Mn(II)(Acetate)₂[Mn(III)(salicylhydroximate)]₄ and (Tetramemthylammonium)₂-[Cu(II)₅(napthoyl-hydroximate)₄], *Inorg. Synth.*, 2002, 33, 70–74.
- 36 D. P. Kessissoglou, J. J. Bodwin, J. Kampf, C. Dendrinou-Samara and V. L. Pecoraro, Pseudohalide complexation by manganese 12-metallacrowns-4 complexes, *Inorg. Chim. Acta*, 2002, **331**, 73–80.
- 37 C. M. Zaleski, S. Tricard, E. C. Depperman, W. Wernsdorfer, T. Mallah, M. L. Kirk and V. L. Pecoraro, Single Molecule Magnet Behavior of a Pentanuclear Mn-Based Metallacrown

- Complex: Solid State and Solution Magnetic Studies, *Inorg. Chem.*, 2011, **50**, 11348–11352.
- 38 C. Atzeri, V. Marzaroli, M. Quaretti, J. R. Travis, L. D. Bari, C. M. Zaleski and M. Tegoni, Elucidation of ¹H NMR Paramagnetic Features of Heterotrimetallic Lanthanide(III)/Manganese(III) 12-MC-4 Complexes, *Inorg. Chem.*, 2017, **56**, 8257–8269.
- 39 E. Lipczynska-Kochany, Photochemistry of Hydroxamic Acids and Derivatives, *Chem. Rev.*, 1991, 91, 477–491.
- 40 E. Galezowska, A. Gluszynska and B. Juskowiak, Luminescence study of G-quadruplex formation in the presence of Tb³⁺ ion, *J. Inorg. Biochem.*, 2007, **101**, 678–685.
- 41 P. L. Thao Tran, E. Largy, F. Hamon, M.-P. Teulade-Fichou and J.-L. Mergny, Fluorescence intercalator displacement assay for screening G4 ligands towards a variety of G-quadruplex structures, *Biochimie*, 2011, **93**, 1288–1296.
- 42 D. Monchaud, C. Allain, H. Bertrand, N. Smargiasso, F. Rosu, V. Gabelica, A. De Cian, J.-L. Mergny and M.-P. Teulade-Fichou, Ligands playing musical chairs with G-quadruplex DNA: A rapid and simple displacement assay for identifying selective G-quadruplex binders, *Biochimie*, 2008, **90**, 1207–1223.
- 43 T. N. Nguyen, C. Y. Chow, S. V. Eliseeva, E. R. Trivedi, J. W. Kampf, I. Martinić, S. Petoud and V. L. Pecoraro, One-Step Assembly of Visible and Near-Infrared Emitting Metallacrown Dimers Using a Bifunctional Linker, *Chem. Eur. J.*, DOI: 10.1002/chem.201703911.